Preprints of the 21st IFAC World Congress (Virtual)
Berlin, Germany, July 12-17, 2020

A Human Inner Ear Model for assessment of Noise Induced Hearing Loss via energy methods

Milka C.I. Madahana * **Otis T.C. Nyandoro** **
John E.D. Ekoru ***

* *School of Electrical and Information Engineering,University of the Witwatersrand, Johannesburg, South Africa(milka.madahana@wits.ac.za).*
** *School of Electrical and Information Engineering,University of the Witwatersrand, Johannesburg, South Africa (otis.nyandoro@wits.ac.za)*
*** *School of Electrical and Information Engineering,University of the Witwatersrand, Johannesburg, South Africa(johnekoru@gmail.com)*

Abstract:
The main objective of this paper is to present a novel Port-Hamiltonian based model of the human inner ear. This model can be used in the assessment and diagnosis of the human inner ear diseases, for instance, Noise Induced Hearing Loss. It may also be used for understanding of sound transmission in the inner ear. The Cochlear Partition is modelled as a pair of Euler-Bernoulli beams coupled together by a linear massless distributed spring. The fluids in the Scala Vestibuli and Scala Tympani are also included in the model. The Cochlear displacement velocity is mainly enhanced by the Outer Hair Cells activities. For frequencies greater than 1 KHz the enhancements become very significant. The developed model also includes the outer hair cells. The model was validated against existing inner ear models and the results were found to be comparable. Future improvements to the model would involve inclusion of the auditory nerve to the model.

Keywords: Port Hamiltonian, Euler Bernoulli, Noise, frequency, Cochlear

1. INTRODUCTION

Exposure to excessive occupational noise may result into permanent hearing loss. Noise Induced Hearing Loss (NIHL) develops slowly over an extended period of time. This period could be months or years. NIHL is a special type of hearing loss that affects the sensory neural hence it falls under the category of sensory neural hearing loss.

When the hearing loss is caused by excessive noise at work, it is then termed as Occupational Noise Induced Hearing Loss (ONIHL). Workers mainly affected by ONIHL are mostly found in the aviation and mining industry. ONIHL is also associated with other health dilemmas, for instance, lack of concentration, irritation, fatigue and sleep disturbance. Not only does this disease affect an individual, it has the ripple effect to the society and the Gross Domestic Production (GDP) of a country Madahana et al. (2019b,c,a).

Some of the details of ONIHL, measurement of threshold shift and ONIHL monitoring system are documented in Madahana et al. (2019b,c,a). It is therefore important for models that can accurately be used in detecting this disease to be developed to allow for an early intervention strategy to be implemented.

2. BACKGROUND

The inner ear is made up of a cochlea which has approximately 8000 hair cells with ostereocilia. When elongated, the cochlea is 30mm long with 0.2 ml cochlea fluid. The cochlea has three parallel canals namely: scala vestibuli, tympani and media. The scala vestibuli is seperated from the Cochlear duct by the vestibular (Reissner's membrane). The basilar membrane divides the Cochlear duct from the scala tympani. Corti is found in the Cochlear duct on the basilar membrane while the tectorial membrane is attached to the roof of organ of corti.

There have been several model developments of the cochlea to aid in investigating the characteristics of the hearing functions that are complex to study and research in vivo because of the cochlea's inaccessibility. Some of the lumped parameter models of the organ of Corti include an active non-linear physiologically based Cochlear model by Lim and Steele (2002). The three dimensional model presented incorporates the viscous fluid effects with an organ of Corti that has a nonlinear active feed forward mechanism. Ramamoorthy et al. (2007) designed a three dimensional finite element cochlea model consisting of electrical, acoustic and mechanical elements. Zhang and Gan (2013) developed a finite element model of the human ear and used it to research the purpose of the middle ear and the cochlea

with respect to the ear structure. Research carried out by Elliott et al. (2013) illustrates the use of the wave finite element method in decomposing the results of a finite element calculation in terms of components. This permits the application of the wave approach using complex numerical methods. Analytical models with an in-depth of the cochlea hydrodynamics have also been provided Reichenbach and Hudspeth (2014). There has been a tremendous change and improvement to the physical models built from Tonndorf (1959), Tonndorf in 1959 to Jang et al. (2015) Micro-Electro-Mechanical Systems(MEMS) based organ of Corti or parts of organ of Corti. Modern advanced technology in measurement systems technology has resulted in micro-mechanical models thus providing evidence that the cochlea is nonlinear and active (Lee et al., 2016). A refined time averaged Lagrangian Cochlear model is developed by Yoon et al. (2009). A Port-Hamiltonian model of a vocal fold fluid structure interaction was reported by Mora et al. (2018).

In order for a proper diagnosis and assessment of the human inner ear to be done accurately and efficiently, there is a need for a suitable model to be developed. Several dynamic models of the inner ear that target other particular conditions rather than NIHL have been developed. NIHL continues to be one of the critical challenges that adversely affects people exposed to loud continuous noise at work, for example mine workers. Port-Hamiltonian model of the ear can be used in assessment and diagnosis of NIHL among mine workers. The Port-Hamiltonian description allows for a more systematic framework for analysing, controlling and simulating intricate physical systems for both distributed and lumped parameter models (van der Schaft, 2006). Therefore, the main contribution in this paper is the development of a novel Port-Hamiltonian model of the human inner ear. The advantages of using Port-Hamiltonian method to model the ear is that it provides a structured way of modelling the ear where components are modelled separately and then interconnected at the end. The ear is made up of three compartments, modelling them separately and then then interconnecting them is much easier. Application of the model developed in this paper are not just limited to NIHL or ONIHL assessment only. The model can be used for other functions as well for instance understanding of sound transmission in the inner ear,development of hearing aids and detection of ear abnormalities. The reminder of the paper is structured as follows: section 1 is the introduction, Section 2 is the background, it is followed by Section 3 which provides the system modelling, Section 4 is the results and discussion and Section 5 is the recommendation and conclusion.

3. SYSTEM MODELLING

Modelling parameters and assumptions taken while developing the Port-Hamiltonian model of the human ear are provided in the subsections that follow.

3.1 Modelling assumptions

The assumptions taken during modelling are stated in this section and repeated in the relevant sections for reference purposes

(1) Assumptions - Scala Vestibula and Scala Tympani:
- The Scala Vestibula and Scala Tympani are modelled as rectangular chambers (Ni et al., 2017; Reichenbach and Hudspeth, 2014; Edom et al., 2014; Beyer, 1992).
- The effect of the convective term in the fluid motion is very small and thus is ignored (Landau and Lidshitz, 1987) .
- The model is concerned with changes about the resting state (equilibrium).
- The fluid is viscous.
- An isentropic fluid assumption is taken so that the navier-stokes equations are given in the velocity-pressure form.
- There is exchange of fluid between the scala vestibula and scala tympani at the helicotrema.

(2) Assumptions - Cochlear Partition:
- The membranes in the Cochlear partition are assumed to deflect only in one direction (such that each cross-section remains perpendicular to its equilibrium position), that is, the Euler Bernoulli assumption. The angular motion about and inline along the equilibrium are assumed to be negligible (Goll and Dalhoff, 2011; Inselberg and Chadwick, 1976).
- The motion at the boundary between the fluid in the scala vestibula and scala tympani Partition and the membranes in the Cochlear Partition is assumed to be very small so that the boundary is not time varying.
- The tectorial membrane and the basilar membrane are interconnected by a distributed spring.

(3) Assumptions - Outer Hair Cells:
- The Outer Hair Cells can be modelled as an simplified equivalent circuit model (Furst, 2015; Cohen and Furst, 2004).

- All boundaries remain constant, that is they do not vary with time. Any displacements at the boundaries of different media are very small and considered negligible.

3.2 Inner ear modelling

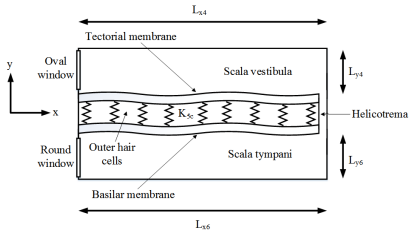

Fig. 1. Model of the inner ear

Scala Vestibula and Scala Tympani fluid The fluid in the Scala Vestibula (S.V.) and the Scala Tympani (S.T.) are modelled using the pressure-velocity form of the Navier Stokes (N.S.) equations without the convective term, $\boldsymbol{v} \cdot \nabla \boldsymbol{v}$, with the addition of fluid viscosity term, $\mu \nabla \cdot \nabla$, to represent the viscous nature of the perilymph fluid in the S.V. and S.T. The N.S. equations with viscosity are (Trenchant et al., 2015)

$$\rho\partial_t \boldsymbol{v} = -\nabla P + \mu\nabla\cdot\nabla\boldsymbol{v}$$
$$\kappa\partial_t P = -\nabla\cdot\boldsymbol{v} \tag{1}$$

The state vector of the P.H. model

$$\boldsymbol{x_i} = \left[\Pi_{x_i}\ \Pi_{y_i}\ \Psi_i\right]^T = \left[\rho_i v_{x_i}\ \rho_i v_{y_i}\ \kappa_i P_i\right]^T \tag{2}$$

where the subscript $i = 4$ and $i = 6$ represent the S.V. and the S.T., respectively, Π_{x_i} and Π_{y_i} are the fluid momenta along the x and $y-$axis directions, respectively, Ψ_i is the fluid stiffness, ρ_i is the fluid density, v_{x_i} and v_{y_i} are the fluid velocities along the x and $y-$axis directions, respectively and κ_i is the fluid compressibility. Taking the time derivative of 2 making the appropriate substitutions into equation 1, the Port-Hamiltonian equations of the fluid in the S.T. and S.V. are given by (Matignon and Hélie, 2013), van der Schaft and Maschke (2002)

$$\partial_t x_i = \left(\mathcal{J}^i - \mathcal{G}_R^i\mathcal{S}^i\mathcal{G}_R^{*i}\right)\left(\delta_{x_i}H_i\right) \tag{3}$$

where

$$\mathcal{J}^i = \begin{bmatrix} 0 & 0 & -\partial_x \\ 0 & 0 & -\partial_y \\ -\partial_x & -\partial_y & 0 \end{bmatrix}, \quad \mathcal{G}_R^i = \left[\partial_x\ \partial_y\ 0\right],$$
$$\mathcal{G}_R^{*i} = -(\mathcal{G}_R^i)^T, \quad \mathcal{S}^i = \mathrm{diag}([\mu_i\ \mu_i\ \mu_i]), \quad e_p^i = Sf_p^i,$$
$$\left(\delta_{x_i}H_i\right) = \mathcal{L}_i x_i = \left[\Pi_{x_i}/\rho_i\ \Pi_{y_i}/\rho_i\ \Psi_i/\kappa_i\right]^T$$

where μ_i is the fluid viscosity, δ_{x_i} is the variational derivative with respect to the state vector, x_i. These equations are obtained from a Hamiltonian

$$H_i\left(x_i\right) = \frac{1}{2}\iint_{\Omega_i} x_i^T\mathcal{L}_i x_i\, dx\, dy \tag{4}$$

where

$$\mathcal{L}_i = \mathrm{diag}([1/\rho_i\ 1/\rho_i\ 1/\kappa_i]) \tag{5}$$

written fully

$$H_i\left(x_i\right) = \frac{1}{2}\int_0^{L_{y_i}}\int_0^{L_{x_i}}\left(\frac{\left(\Pi_{x_i}\right)^2}{\rho_i} + \frac{\left(\Pi_{y_i}\right)^2}{\rho_i} + \frac{\left(\Psi_i\right)^2}{\kappa_i}\right) dx\, dy$$

The time derivative of the Hamiltonian

$$\begin{aligned}\partial_t H_i &= \iint_\Omega x_i^T\mathcal{L}\left(\partial_t x_i\right)\, d\Omega \\ &= \iint_\Omega x_i^T\mathcal{L}\left(\mathcal{J}^i - \mathcal{G}_R^i\mathcal{S}^i\mathcal{G}_R^{*i}\right)\left(\delta_{x_i}H_i\right)\, d\Omega\end{aligned} \tag{6}$$

so that the Dirac structure is given by (Trenchant et al., 2015):

$$\begin{aligned}\langle e^1, (\mathcal{J} - \mathcal{G}_R\mathcal{S}\mathcal{G}_R^*)e^2\rangle &= \iint_\Omega \left(e^1\right)^T\left(\mathcal{J} - \mathcal{G}_R\mathcal{S}\mathcal{G}_R^*\right)e^2\, d\Omega \\ = -\int_0^{L_x}\left[e_2e_3 + e_3e_2\right]_0^{L_y} dx - \int_0^{L_y}\left[e_1e_3 + e_3e_1\right]_0^{L_x} dy \\ + \iint_\Omega \left[e_1\partial_x e_3 + e_2\partial_y e_3 + e_3\partial_x e_1 + e_3\partial_y e_2\right] d\Omega \\ + \int_0^{L_x}\mu\left[e_1\partial_x e_2 + e_2\partial_y e_2\right]_0^{L_y}\, dx + \int_0^{L_y}\mu\left[e_1\partial_x e_1\right. \\ \left. + e_2\partial_y e_1\right]_0^{L_x}\, dy - \iint_\Omega \mu\left[\partial_x e_1\partial_x e_2 + \partial_x e_2\partial_y e_2\right. \\ \left. + \partial_y e_1\partial_x e_1 + \partial_y e_2\partial_y e_2\right]\, d\Omega\end{aligned} \tag{7}$$

where $e^1 = e^2 = \left[e_1\ e_2\ e_3\right]^T$. Furthermore,

$$\langle e^1, (\mathcal{J} - \mathcal{G}_R\mathcal{G}_R^*\mathcal{S})e^2\rangle = -\langle -(\mathcal{J} - \mathcal{G}_R\mathcal{G}_R^*\mathcal{S})e^1, e^2\rangle \tag{8}$$

Cochlear Partition The Cochlear Partition (C.P.) is modelled as a pair of Euler-Bernoulli beams coupled together by a linear massless distributed spring of stiffness $K_{5_{ab}}$. The C.P.'s equations of motion are expressed as (Villegas, 2007; Furst, 2015):

$$\begin{aligned}\rho_{5_a}\partial_t^2 v_{5_a} &= -\partial_x^2\left(EI_{5_a}\partial_x^2 v_{5_a}\right) - B_{5_a}\partial_t v_{5_a} \\ &\quad -K_{5_{ab}}\left(v_{5_a} - v_{5_b}\right) \\ \rho_{5_b}\partial_t^2 v_{5_b} &= -\partial_x^2\left(EI_{5_b}\partial_x^2 v_{5_b}\right) - B_{5_b}\partial_t v_{5_b} \\ &\quad +K_{5_{ab}}\left(v_{5_a} - v_{5_b}\right)\end{aligned} \tag{9}$$

where $\rho_{(\cdot)}$ is density per unit length, $v_{(\cdot)}$ is the transverse deflection of the beam, $EI_{(\cdot)}$ is flexural rigidity and $B_{(\cdot)}$ is viscous damping. The subscripts 5, 5_a and 5_b are used to indicate the Cochlear Partition and the Tectorial and Basilar membranes, respectively. The Port-Hamiltonian state vector of the C.P., x_5, is

$$x_5 = \left[\Pi_{5_a}\ \Psi_{5_a}\ \Pi_{5_b}\ \Psi_{5_b}\ \Phi_{5_{ab}}\right]^T \tag{10}$$

where $\Pi_{5_{(\cdot)}} = \rho_{5_{(\cdot)}}\partial_t v_{5_{(\cdot)}}$ and $\Psi_{5_{(\cdot)}} = \partial_x^2 v_{5_{(\cdot)}}$ are is the momentum and curvature of the membranes, respectively and $\Phi_{5_{ab}}$ is the relative displacement between the tectorial and basilar membranes. $\Phi_{5_{ab}}$ is calculated by integrating the difference in membrane velocities

$$\partial_t\Phi_{5_{ab}} = \Pi_{5_a}/\rho_{5_a} - \Pi_{5_b}/\rho_{5_b} \tag{11}$$

Taking the time derivative of the state vector x_5, making the appropriate substitutions into equation 9, the equations of the C.P. in terms of the P.H. states become

$$\begin{aligned}\partial_t\Pi_{5_a} &= -\partial_x^2 EI_{5_a}\Psi_{5_a} - B_{5_a}\Pi_{5_a}/\rho_{5_a} - K_{5_{ab}}\Phi_{5_{ab}} \\ \partial_t\Psi_{5_a} &= \partial_x^2\Pi_{5_a}/\rho_{5_a} \\ \partial_t\Pi_{5_b} &= -\partial_x^2 EI_{5_b}\Psi_{5_b} - B_{5_b}\Pi_{5_b}/\rho_{5_b} + K_{5_{ab}}\Phi_{5_{ab}} \\ \partial_t\Psi_{5_b} &= \partial_x^2\Pi_{5_b}/\rho_{5_b}\end{aligned} \tag{12}$$

Equation 12 can be derived from the Hamiltonian

$$H_5\left(x_5\right) = \frac{1}{2}\int_a^b x_5^T\mathcal{L}_5 x_5\, dx \tag{13}$$

where (Villegas, 2007)

$$\mathcal{L}_5 = \text{diag}([1/\rho_{5_a}\ \ EI_{5_a}\ \ 1/\rho_{5_b}\ \ EI_{5_b}\ \ K_{5_{ab}}])$$

written out in full

$$H_5(x_5) = \frac{1}{2}\int_0^{L_{x_5}} \left(\frac{(\Pi_{5_a})^2}{\rho_{5_a}} + EI_{5_a}(\Psi_{5_a})^2 + \frac{(\Pi_{5_b})^2}{\rho_{5_b}} + EI_{5_b}(\Psi_{5_b})^2 + K_{5_{ab}}(\Phi_{5_{ab}})^2 \right) dx$$

The P.H. model of the C.P. is

$$\begin{aligned} \partial_t x_5 &= \left(\mathcal{J}_5 - \mathcal{G}_R^5 \mathcal{S}^5 \mathcal{G}_R^{*5}\right)(\delta_{x_5} H_5) + G_I^5 u_5 \\ y_5 &= G_I^{*5}(\delta_{x_5} H_5) \end{aligned} \tag{14}$$

where

$$\mathcal{J}_5 = P_0^5 + P_1^5 \partial_x + P_2^5 \partial_x^2,$$

$$P_0^5 = P_1^5 = \text{diag}([0\ 0\ 0\ 0\ 0]), \quad P_2^5 = \begin{bmatrix} 0 & -1 & 0 & 0 & 0 \\ 1 & 0 & 0 & 0 & 0 \\ 0 & 0 & 0 & -1 & 0 \\ 0 & 0 & 1 & 0 & 0 \\ 0 & 0 & 0 & 0 & 0 \end{bmatrix},$$

$$\mathcal{G}_R^5 = \text{diag}([1\ 0\ 1\ 0\ 0]), \quad \mathcal{G}_R^{*5} = -(\mathcal{G}_R^5)^T,$$

$$\mathcal{S}_5 = -\text{diag}([B_{5_a}\ \ 0\ \ B_{5_b}\ \ 0\ \ 0]),$$

$$(\delta_{x_5} H_5) = \mathcal{L}_5 x_5 = \begin{bmatrix} \Pi_{5_a}/\rho_{5_a} \\ EI_{5_a}\Psi_{5_a} \\ \Pi_{5_b}/\rho_{5_b} \\ EI_{5_b}\Psi_{5_b} \\ K_{5_{ab}}\Phi_{5_{ab}} \end{bmatrix}, G_I^5 = \begin{bmatrix} 1 & 0 \\ 0 & 0 \\ 0 & 1 \\ 0 & 0 \\ 0 & 0 \end{bmatrix}, u_5 = \begin{bmatrix} u_{5_a} \\ u_{5_b} \end{bmatrix}$$

The boundary ports are

$$\begin{bmatrix} f_\partial \\ e_\partial \end{bmatrix} = \frac{1}{\sqrt{2}} \begin{bmatrix} Q_5 & -Q_5 \\ I & I \end{bmatrix} \begin{bmatrix} \delta_{x_5} H_5(b) \\ \delta_{x_5} H_5(a) \end{bmatrix}, \text{ where } Q_5 = P_2^5$$

3.3 Model Interconnection

The inner ear interconnection is described below:

Scala Vestibula and Tectorial membrane

- The momentum of the Scala Vestibula fluid, Θ_4, is equal to the momentum of the Tectorial membrane at their interface:

$$\Theta_4(t, x, 0) = \Pi_{5_a}(t, x) \tag{15}$$

- The force of the Tectorial membrane, F_{5_a}, is equal to the fluid pressure per unit area applied by the Scala Vestibula at their interface:

$$F_{5_a}(t, x) = \frac{\Psi_4(t, 0, y)}{A_{5_a}} \tag{16}$$

assuming the area of contact remains constant.

Scala Tympani and Basilar Membrane :

- The momentum of the Scala Tympani fluid, Θ_6, is equal to the momentum of the Basilar membrane at their interface:

$$\Theta_6(t, x, L_y) = \Pi_{5_b}(t, x) \tag{17}$$

- The force of the Basilar membrane, F_{5_b}, is equal to the fluid pressure per unit area applied by the Scala Tympani at their interface:

$$F_{5_b}(t, x) = \frac{\Psi_6(t, L_x, y)}{A_{5_b}} \tag{18}$$

assuming the area of contact remains constant.

Helicotrema

- The fluid momentum and pressure of the Scala Vestibula and Scala Tympani are equal at the helicotrema.

$$\Theta_4(t, L_x, 0) = \Theta_6(t, L_x, L_y) \tag{19}$$

$$\Psi_4(t, L_x, 0) = \Psi_6(t, L_x, L_y) \tag{20}$$

3.4 Modelling Parameters

Table 1 to Table 3 provides the modelling parameters.

4. INNER EAR SIMULATION RESULTS AND DISCUSSION

The derived Port-Hamiltonian equations of a human adult inner ear with normal hearing is simulated. The model was implemented using MATLAB as a modelling platform and the results were generated using the Simulink

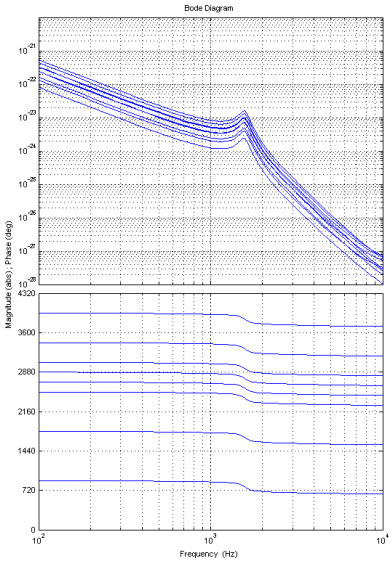

Fig. 2. Cochlear frequency response

The sensitivity of the human ear changes as a function of frequency. Figure 2 shows the Sound Pressure Level (SPL) required for the frequencies to be perceived as loud. When sensorineural hearing loss (damage to the cochlea) is present, the perception of loudness is altered. Typically hearing tests are performed over a range of frequencies for instance from 250 to 8000 Hz. The hearing threshold is measured in decibels relative to the normal threshold. Hearing loss is caused by a dip near the 4000 Hz.

4.1 Outer Hair Cell modelling

Given the Perilymph has a resting potential $\psi_{5_{d0}}$, the Outer Hair Cells are modelled based on an the equivalent circuit model method as shown in Figure 3 (Furst, 2015; Cohen and Furst, 2004).

Table 1. Basilar Membrane (Gan et al., 2006, 2004)

Parameter	Symbol	Value
Density	ρ_{BM}	$1.2g/cm^3$
Young's Modulus (base to middle)	EI_{BM}	$[50 \times 10^{11}, 15 \times 10^{11}]g \cdot cm/s^2$
Young's Modulus (middle to apex)	EI_{BM}	$[15 \times 10^{11}, 3 \times 10^{11}]g \cdot cm/s^2$
Damping (base to apex)	β_{BM}	$[0.2 \times 10^{-3}, 0.1 \times 10^{-2}]g \cdot cm/s^2$

Table 2. Scala Vestibula and Scala Tympani Fluid (Water at 20° Celcius) (Gan et al., 2006, 2004)

Parameter	Symbol	Value
Density	$\rho_{\mathrm{SV}}, \rho_{\mathrm{ST}}$	$9.982 \times 10^{-1} g/cm^3$
Speed of sound	$c_{\mathrm{SV}}, c_{\mathrm{ST}}$	$1.45 \times 10^5 cm/s$
Kinematic viscosity	$\nu_{\mathrm{SV}}, \nu_{\mathrm{ST}}$	$1.003 \times 10^{-5} cm^2/s$

$$\partial_t \psi_{5_d} = \omega_{5_d}(\psi_{5_d} - \psi_{5_{d0}}) + \eta_{5_d}\phi_{5_{ab}} \tag{21}$$

where ψ_{5_d} and ω_{5_d} are the voltage and cut-off frequency of the OHC surface, respectively, η_{5_d} is a constant conversion factor and $\phi_{5_{ab}}$ is the relative displacement of the Basilar and Tectorial membranes. $\phi_{5_{ab}}$ is obtained by integrating $\Phi_{5_{ab}}$.

The Port-Hamiltonian state vector of the OHC is x_{5_d}

$$x_{5_d} = [\Psi_{5_d}] = [\psi_{5_d}] \tag{22}$$

The Hamiltonian function H_{5_d} is given by

$$H_{5_d} = \frac{1}{2}\omega_{5_d}(\Psi_{5_d} - \Psi_{5_{d0}})^2 \tag{23}$$

The P.H. model of the OHC is

$$\partial_t x_{5_d} = \mathcal{J}_{5_d}(\delta_{5_d} H_{5_d}) + G_{5_d} u_{5_d} \tag{24}$$

$$y_{5_d} = G_I^{*5_d}(\delta_{5_d} H_{5_d}) \tag{25}$$

The pressure applied by the OHC onto the Basilar and Tectorial membranes P_{ohc} is (Furst, 2015; Cohen and Furst, 2004)

$$P_{ohc}(x,t) = K_{5_{ab}}(\phi_{5_{ab}} - \Delta_{ohc}) \tag{26}$$

where Δ_{ohc} is the deflection of the outer hair cell Furst (2015); Cohen and Furst (2004)

$$\Delta_{ohc} = \alpha_s \tanh(-\alpha x_{5_d}) \tag{27}$$

where α_1 and α_s are the reference voltage and peak to peak deflection due to electro-mobility.

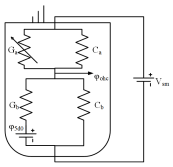

Fig. 3. Outer Hair Cell electrical circuit model (Furst, 2015; Cohen and Furst, 2004)

4.2 Outer Hair Cell results and discussion

Figure 4 shows the frequency response of the OHC at 0.3889cm, 1.1667cm, 1.9444cm, 2.7222cm and 3.5cm from the base of the Cochlear. The cochlear displacement velocity is mainly enhanced by the OHC activities. For frequencies that are greater than 1 KHz which is the cutoff frequency of the OHCs membrane, the enhancement becomes very significant. The basilar membrane motion is very sensitive to the any change in the gain of the OHCs. ONIHL is traditionally observed by an audiogram whose maximum threshold shift occurs at 4KHz. This model is consistent with the assumption by Furst (2015); Cohen and Furst (2004) and is further supported by current research that indicates that the loss in hearing sensitivity in humans that occurs at 4 KHz is independent of the type of noise exposure (Furst, 2015; Cohen and Furst, 2004). Presbycusis is characterized by hearing loss at high frequencies. The proposed Port-Hamiltonian model only deals with OHC hearing loss. It is therefore assumed that the loss of IHC that usually follows OHC loss is the cause of profound hearing loss. The Port-Hamiltonian results of the OHCs were validated against Furst (2015); Cohen and Furst (2004) and were found to be comparable and followed a similar pattern of behaviour (Furst, 2015; Cohen and Furst, 2004).

Table 3. Outer Hair Cells (Furst, 2015; Cohen and Furst, 2004)

Parameter	Symbol	Value
Peak to peak electromotile deflection	α_{s}	$1 \times 10^{-6} cm$
Reference electromotile voltage	α_{l}	$2 \times 10^{-6} V$
Cut-off frequency	ω_{ohc}	$2\pi \times 10^3 rad/s$
Resting potential of Periylymph	$\psi_{5_{d0}}$	$-7 \times 10^{-2} V$

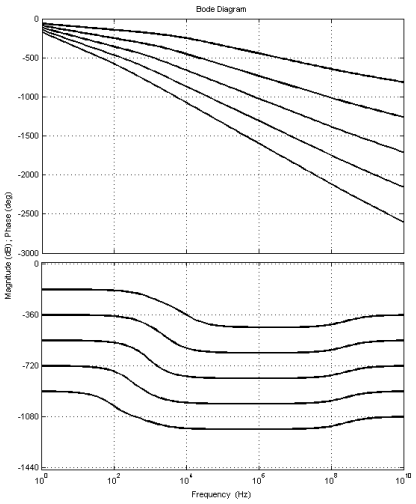

Fig. 4. Outer Hair Cell frequency response, at the points 0.3889cm, 1.1667cm, 1.9444cm, 2.7222cm and 3.5cm from the base of the Cochlear

5. RECOMMENDATIONS AND CONCLUSION

To improve these work in future, the following will be added to the system: The cochlea will be modelled as a fluid filled, snail shaped cavern, a comprehensive Port-

Hamiltonian model of the human ear including the outer and middle ear will be developed for sound transmission and the auditory nerve will be included to see the complete cycle of sound transmission. In conclusion, a comprehensive model of the human inner ear has been presented. This model is useful in the diagnosis and assessment of the inner ear pathologies. Noise Induced Hearing loss has been used to illustrate the significance of this model. The Port-Hamiltonian model of the human inner ear developed also includes inner hair cells which are usually used to determine whether an individual has ability to hear or not.

REFERENCES

Beyer, R.P. (1992). A computational model of the Cochlea using the immersed boundary method. *Journal of Computational Physics*, 98(1), 145–162.

Cohen, A. and Furst, M. (2004). Integration of Outer Hair Cell activity in a one-dimensional Cochlear model. *The Journal of the Acoustical Society of America*, 115(5), 2185–2192.

Edom, E., Obrist, D., and Kleiser, L. (2014). Steady streaming in a two-dimensional box model of a passive Cochlear. *Journal of Fluid Mechanics*, 753, 254–278.

Elliott, S.J., Ni, G., Mace, B.R., and Lineton, B. (2013). A wave finite element analysis of the passive Cochlea. *The Journal of the Acoustical Society of America*, 133(3), 1535–1545.

Furst, M. (2015). Cochlear model for hearing loss. In F. Bahmad Jr. (ed.), *Update On Hearing Loss*, chapter 1. IntechOpen, Rijeka.

Gan, R.Z., Suna, Q., Feng, B., and Wood, M.W. (2006). Acoustic-structural coupled Finite Element analysis for sound transmission in Human Ear-pressure distributions. *Medical Engineering and Physics*, 28(5), 395 – 404.

Gan, R.Z., Feng, B., and Sun, Q. (2004). Three-dimensional finite element modeling of Human ear for sound transmission. *Annals of Biomedical Engineering*, 32(6), 847–859.

Goll, E. and Dalhoff, E. (2011). Modeling the Eardrum as a string with distributed force. *The Journal of the Acoustical Society of America*, 130(3), 1452–1462.

Inselberg, A. and Chadwick, R.S. (1976). Mathematical model of the Cochlea I: Formulation and solution. *SIAM Journal on Applied Mathematics*, 30(1), 149–163.

Jang, J., Lee, J., Woo, S., Sly, D.J., Campbell, L.J., Cho, J.H., O'Leary, S.J., Park, M.H., Han, S., Choi, J.W., Jang, J.H., and Choi, H. (2015). A microelectromechanical system artificial Basilar membrane based on a piezoelectric cantilever array and its characterization using an animal model. *Scientific reports*, 5, 12447.

Landau, L.D. and Lidshitz, E.M. (1987). *Fluid Mechanics*. Pergamon Press, Oxford, England, 2nd edition.

Lee, H.Y., Raphael, P.D., Xia, A., Kim, J., Grillet, N., Applegate, B.E., Bowden, A.K.E., and Oghalai, J.S. (2016). Two-dimensional cochlear micromechanics measured in vivo demonstrate radial tuning within the Mouse organ of Corti. *Journal of Neuroscience*, 36, 8160–8173.

Lim, K.M. and Steele, C.R. (2002). A three-dimensional nonlinear active Cochlear model analyzed by the WKB-numeric method. *Hearing Research*, 170(1), 190 – 205. Special Issue on the 38th Workshop on Inner Ear Biology , and regular research papers.

Madahana, M., Ekoru, J., Mashinini, T., and Nyandoro, O. (2019a). Noise level policy advising system for mine workers. *IFAC-PapersOnLine*, 52, 249–254.

Madahana, M., Ekoru, J., and Nyandoro, O. (2019b). Smart automated noise policy monitoring and feedback control system for mining application. *IFAC-PapersOnLine*, 52, 177–182.

Madahana, M.C., Ekoru, J.E., Mashinini, T.L., and Nyandoro, O.T. (2019c). Mine workers threshold shift estimation via optimization algorithms for deep recurrent neural networks. *IFAC-PapersOnLine*, 52(14), 117–122.

Matignon, D. and Hélie, T. (2013). A class of damping models preserving eigenspaces for linear conservative Port-Hamiltonian systems. *European Journal of Control*, 19(6), 486 – 494. Lagrangian and Hamiltonian Methods for Modelling and Control.

Mora, L.A., Yuz, J.I., Ramirez, H., and Le Gorrec, Y. (2018). A Port-Hamiltonian fluid-structure interaction model for the vocal. *IFAC-PapersOnLine*, 51(3), 62 – 67.

Ni, G., Sun, L., and Elliott, S.J. (2017). A linearly tapered box model of the Cochlear. *The Journal of the Acoustical Society of America*, 141(3), 1793–1803.

Ramamoorthy, S., Deo, N.V., and Grosh, K. (2007). A mechano-electro-acoustical model for the Cochlea: Response to acoustic stimuli. *The Journal of the Acoustical Society of America*, 121(5), 2758–2773.

Reichenbach, T. and Hudspeth, A.J. (2014). The physics of hearing: fluid mechanics and the active process of the Inner Ear. *Reports on progress in Physics*, 77(7), 076601.

Tonndorf, J. (1959). Beats in cochlear models. *The Journal of the Acoustical Society of America*, 31, 124.

Trenchant, V., Fares, Y., Ramirez, H., Le Gorrec, Y., and Ouisse, M. (2015). A Port-Hamiltonian formulation of a 2D boundary controlled acoustic system. *IFAC-PapersOnLine*, 48(13), 235240.

van der Schaft, A. (2006). Port-Hamiltonian systems: an introductory survey. suppl 2, 1339–1365. European Mathematical Society Publishing House (EMS Ph).

van der Schaft, A. and Maschke, B. (2002). Hamiltonian formulation of distributed-parameter systems with boundary energy flow. *Journal of Geometry and Physics*, 42(1), 166 – 194.

Villegas, J.A. (2007). *A Port-Hamiltonian Approach to Distributed Parameter Systems*. Ph.D. thesis, Department of Applied Mathematics, Faculty EWI, Universiteit Twente, Enschede, Twente, Enschede, Netherlands.

Yoon, Y., Puria, S., and Steele, C.R. (2009). A Cochlear model using the time-averaged Lagrangian and the push-pull mechanism in the organ of Corti. *Journal of mechanics of materials and structures*, 4, 977–986.

Zhang, X. and Gan, Z.R. (2013). Finite element modeling of energy absorbance in normal and disordered Human Ears. *Hearing Research*, 301, 146 – 155. MEMRO 2012 - Middle-Ear Bridge between Science and Otology.